

# Exploring the In Situ Formation Mechanism of Polymeric Aluminum Chloride–Silica Gel Composites under Mechanical Grinding Conditions: As a High-Performance Nanocatalyst for the Synthesis of Xanthene and Pyrimidinone Compounds

Gang Wang, Yage Geng, Zejing Zhao, Qiuping Zhang, Xiang Li, Zhiqiang Wu, Shuxian Bi, Haijuan Zhan,\* and Wanyi Liu\*



Cite This: *ACS Omega* 2022, 7, 32577–32587



Read Online

ACCESS |



Metrics & More



Article Recommendations



Supporting Information

**ABSTRACT:** The use of mechanical ball milling to facilitate the synthesis of organic compounds has attracted intense interest from organic chemists. Herein, we report a new process for the preparation of xanthene and pyrimidinone compounds by a one-pot method using polymeric aluminum chloride (PAC), silica gel, and reaction raw materials under mechanical grinding conditions. During the grinding process, polymeric aluminum chloride and silica gel were reconstituted in situ to obtain a new composite catalyst (PAC–silica gel). This catalyst has good stability (six cycles) and wide applicability (22 substrates). The Al–O–Si active center formed by in situ grinding recombination was revealed to be the key to the effective catalytic performance of the PAC–silica gel composites by the comprehensive analysis of the catalytic materials before and after use. In addition, the mechanism of action of the catalyst was verified using density functional theory, and the synthetic pathway of the xanthene compound was reasonably speculated with the experimental data. Mechanical ball milling serves two purposes in this process: not only to induce the self-assembly of silica and PAC into new composites but also to act as a driving force for the catalytic reaction to take place. From a practical point of view, this “one-pot” catalytic method eliminates the need for a complex preparation process for catalytic materials. This is a successful example of the application of mechanochemistry in materials and organic synthesis, offering unlimited possibilities for the application of inorganic polymer materials in green synthesis and catalysis promoted by mechanochemistry.



## 1. INTRODUCTION

In the 21st century, chemistry has brought unlimited possibilities to human life, but the pollution produced by chemical manufacturing processes is also very difficult to solve.<sup>1</sup> The greening of chemical production processes is attracting wider attention from scientists.<sup>2</sup> Among them, the reaction process and the product purification process are the most serious pollution stages because they require the use of large amounts of solvents. Many research groups have contributed to the greening of both processes and achieved good results.<sup>2–4</sup> The mechanochemical synthesis of organic molecules offers the advantages of a simple operating technique, low energy consumption, decreased waste treatment, and ease of large-scale manufacturing.<sup>5–8</sup> Because mechanochemistry does not require the use of solvents in the reaction process, it has been hailed as one of the most promising technologies for green synthesis and catalysis.<sup>9–13</sup> While mechanochemistry often brings unexpected surprises to researchers in terms of results, the mechanism of catalysis in

the process is still like a “black box” full of uncertainties. For this reason, it is important to investigate the reaction process in detail and to reveal the reaction mechanism.<sup>14–16</sup>

Poly(aluminum chloride) (PAC), as an inorganic high molecular polymer with a unique polynuclear Al–O structure and distinctive electrical properties, is frequently utilized in the flocculation process of water treatment.<sup>17–20</sup> PAC materials can be produced from ore materials or chemical waste and have the advantages of being simple to prepare, widely available, and inexpensive. Because of its rich metal cation structure (sites of Lewis acid), poly(aluminum chloride) has been shown to be a reliable and ecologically acceptable catalyst

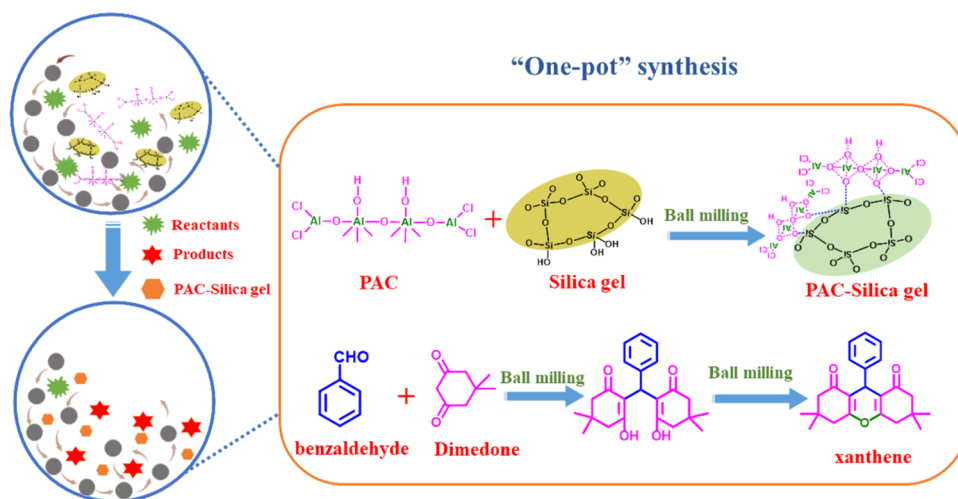
Received: July 2, 2022

Accepted: August 19, 2022

Published: August 30, 2022



## Scheme 1. One-Step Synthesis of Xanthene Compounds Assisted by Mechanical Ball Milling



for the production of bis-indolemethane and pyrimidinone molecules.<sup>21,22</sup> However, there are still issues with metal loss and solvent recovery challenges. The clever combination of PAC materials with mechanochemistry has the potential to tackle the challenges mentioned above while also bringing fresh ideas for its application in catalysis.

In recent years, researchers have been working on a variety of novel catalysts for synthesis and catalysis.<sup>23–25</sup> However, most research just reported on its catalytic phenomena and did not go into detail on its catalytic mechanism, whether from the standpoint of the reaction or catalyst. This severely limits the application of these materials because of their unclear mechanism of action. The development of density functional theory (DFT) has opened up new possibilities for the advancement of conventional chemistry, particularly catalytic chemistry.<sup>26–28</sup> Using the data simulation method, the reaction paths of different catalysts can be calculated so that the mechanism of action of the catalysts can be more clearly shown to the researchers.<sup>29</sup> The combination of density functional theory and experimental data may expose the catalyst's mechanism in the synthesis and catalysis processes in great detail, as well as give theoretical advice for the future development of this type of catalyst.

Here, we provide a novel approach for synthesizing xanthene and pyrimidine fused ring compounds by combining the reaction raw materials, PAC, and silica gel in a mechanical grinder at room temperature (Scheme 1). The catalytic process has the advantages of being a green process and having convenient operation, quick separation and purification of products, and easy large-scale production. Due to the uncertainty of the catalytic mechanism during mechanical ball milling, the materials were characterized using scanning electron microscopy (SEM), high-resolution transmission electron microscopy (HRTEM), X-ray photoelectron spectroscopy (XPS), and Fourier transform infrared (FTIR) spectra tests to explore the catalytic active sites. The catalytic mechanism of PAC and silica gel in the "one-step" synthesis of xanthene compounds was also elucidated by combining step-by-step reaction control and density functional theory simulations. This research work will lay a theoretical foundation for the broader development of inorganic polymer materials represented by PAC in the field of green synthesis and catalysis.

## 2. EXPERIMENTAL SECTION

**2.1. General Methods.** All reagents are more than 98% pure and the solvent is A.R. <sup>1</sup>H and <sup>13</sup>C NMR were recorded by a Bruker 400 MHz spectrometer. Scanning electron microscopy (Zeiss Sigma 300), high-resolution transmission electron microscopy (FEI Tecnai G2 F20), X-ray photoelectron spectroscopy (Thermo Scientific K-Alpha), density functional theory simulations (supported by Shiyanjia Lab ([www.shiyanjia.com](http://www.shiyanjia.com)) using Vienna Ab initio Simulation Package (VASP) software) were used in the paper.

**2.2. Typical Procedure for the Synthesis of 1,8-Dioxaoctahydroanthracene Compounds.** 4-Nitrobenzaldehyde (1.0 mmol), 5,5-dimethyl-1,3-cyclohexanedione (2.0 mmol), silica gel (0.4 g), and PAC (0.05 g) were added to a grinder and ground at 50 Hz for a certain period of time, and thin-layer chromatography (TLC) was used to monitor the reaction. After the reaction, the reaction mixture was dissolved in ethyl acetate (3 × 5 mL) and filtered. The filtrate was concentrated and purified by recrystallization from ethanol to obtain the product. The filtered solid mixture was dried and then used for the next reaction.

## 3. RESULTS AND DISCUSSION

**3.1. Catalytic Tests.** 1,8-Dioxaoctahydroanthracene compounds have extremely high pharmacological activity and use value in the fields of dyes and photosensitive materials and are antibacterial and anti-inflammatory, so they are considered to be the most practical type of heterocyclic compounds.<sup>30</sup> In recent years, many catalysts utilized to catalyze the formation of heteroanthracene molecules have been widely reported.<sup>31–34</sup> However, need toxic solvents, metal loss pollutes water, harsh reaction conditions, the amount of catalyst used is enormous and cannot be recovered, and the low product yield persists.<sup>35–37</sup> In this work, affordable and industrially manufactured poly(aluminum chloride) and silica gel were utilized as catalysts, and heteroanthracene compounds were prepared using a one-pot process under mechanical grinding. The catalytic activity of different catalysts is shown in Figure 1. First, simple mechanical grinding does not promote the reaction, which indicates that a catalyst is necessary. The conversion rate of raw materials is 10% when PAC is employed alone as a catalyst, but no target product is generated. Silica gel can convert 80% of the raw materials, but there is still no final

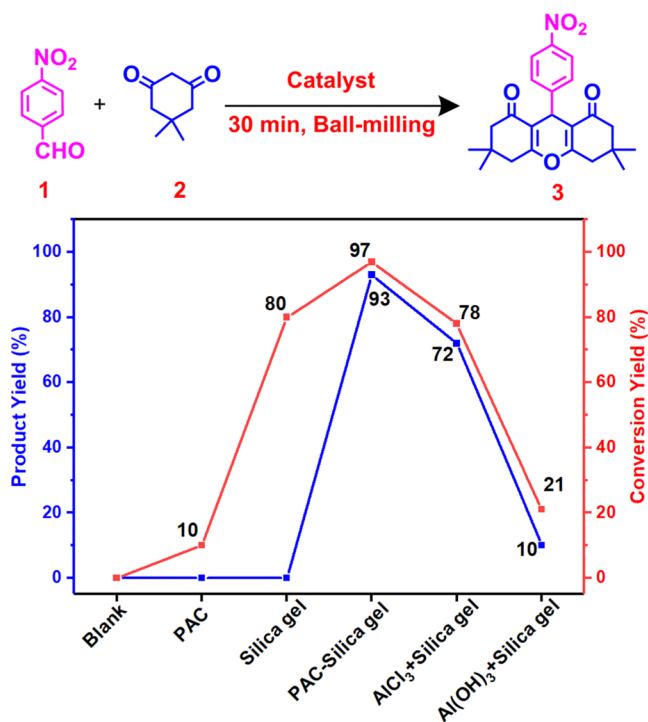


**Figure 1.** Catalytic activity of different catalysts in the synthesis of xanthene compounds: 4-nitrobenzaldehyde (1.0 mmol), 5,5-dimethyl-1,3-cyclohexanedione (2.0 mmol), silica gel (0.4 g), and PAC (0.05 g).

product. This indicates that silica gel serves as a cocatalyst in addition to dispersing in the grinding process, and it can promote the conversion of raw materials. The conversion rate of the raw materials was 97% when PAC and silica gel were added to the reaction and milled for 24 min, and the yield of the target compound was 93%. This encouraging finding indicates that PAC and silica gel have a synergistic catalytic effect and that they may form new catalytic active centers during grinding. Furthermore, instead of PAC components, aluminum chloride and aluminum hydroxide are employed, and their catalytic reaction activity is lower than PAC's. This indicates that the special polynuclear Al–O cation structure of the PAC material plays a key role in the catalytic process (the detailed screening results of reaction conditions are shown in Table S1).

The use of a combination of mechanical grinding and chemical reaction overcomes the problem of reaction kinetics, and the process does not need the use of solvents, which effectively avoids the corrosion of equipment caused by organic solvents in traditional reactions. The catalytic activity of the gram-scale reaction was investigated when it was ramped up to 10 mmol (Figure 2). The desired compound was achieved with a 93% yield after 30 min of grinding. The catalyst can be recovered following simple filtering using ethyl acetate-dissolved products. After six times of usage, the PAC–silica gel catalyst still exhibits strong catalytic activity (yield = 93%). The grinding time required to complete the reaction increased slightly during the recycling process, but it was still completed in under an hour (Table S2). Furthermore, it is very worth mentioning that the product can be created by ethanol recrystallization, and the ethanol used in the recrystallization process can be recovered and reused. This finding provides the

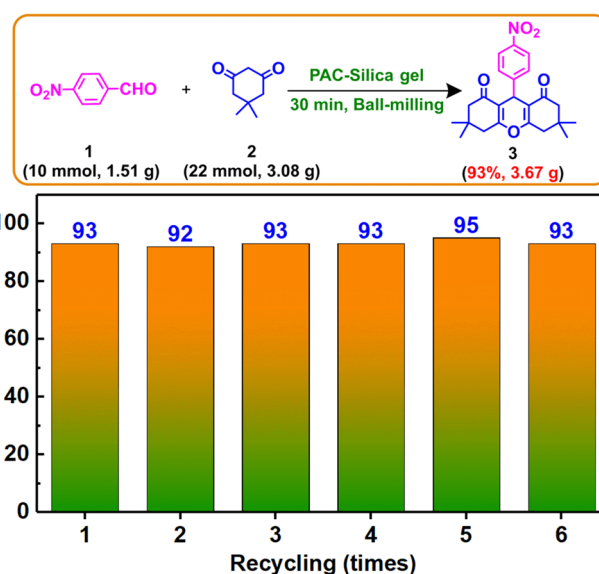
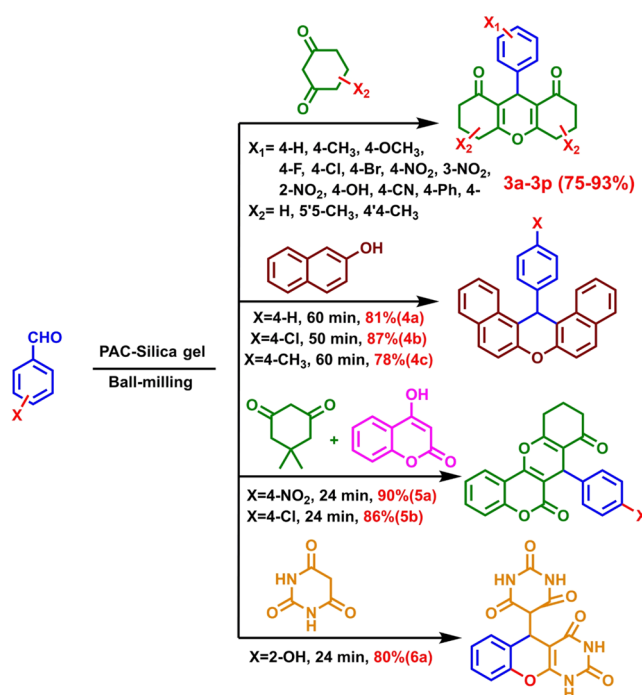


**Figure 2.** Reuse and gram-scale preparation reaction by the PAC–silica catalyst.

possibility for the industrial application of this one-pot approach for preparing xanthene compounds.

The synthesis of other substituent groups and three other pyrimidinone ring compounds was undertaken to further validate the universality of the PAC–silica gel catalyst, and satisfactory results were obtained (Scheme 2). The PAC–silica gel catalyst has shown excellent catalytic activity in four types of reactions (synthesis of 20 different substrates, Table S3). This is due to the special combination of PAC and silica gel in the mechanical grinding process. PAC and silica gel form new catalytic active centers in situ under the action of mechanical

### Scheme 2. Synthesis of Heteranthrene Compounds by the PAC–Silica Gel Catalyst under Mechanical Grinding Conditions



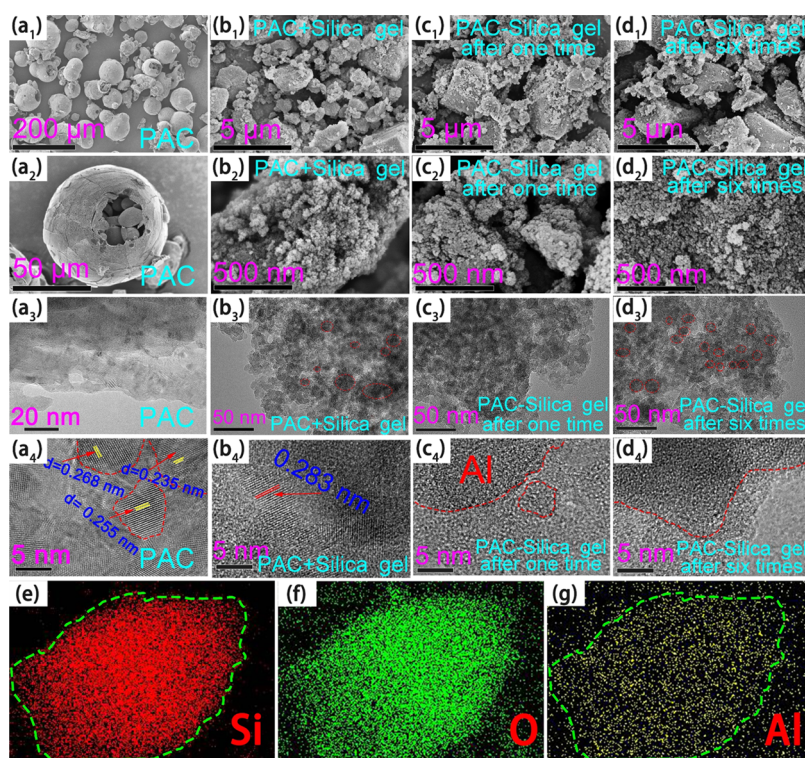


**Figure 3.** SEM and HRTEM image of (a<sub>1</sub>–a<sub>4</sub>) PAC catalysts; (b<sub>1</sub>–b<sub>4</sub>) PAC + silica gel before use; (c<sub>1</sub>–c<sub>4</sub>) PAC–silica gel after one time; and (d<sub>1</sub>–d<sub>4</sub>) PAC–silica gel after six times. (e–g) Energy dispersive spectrometry (EDS) mapping of PAC–silica gel after one time.

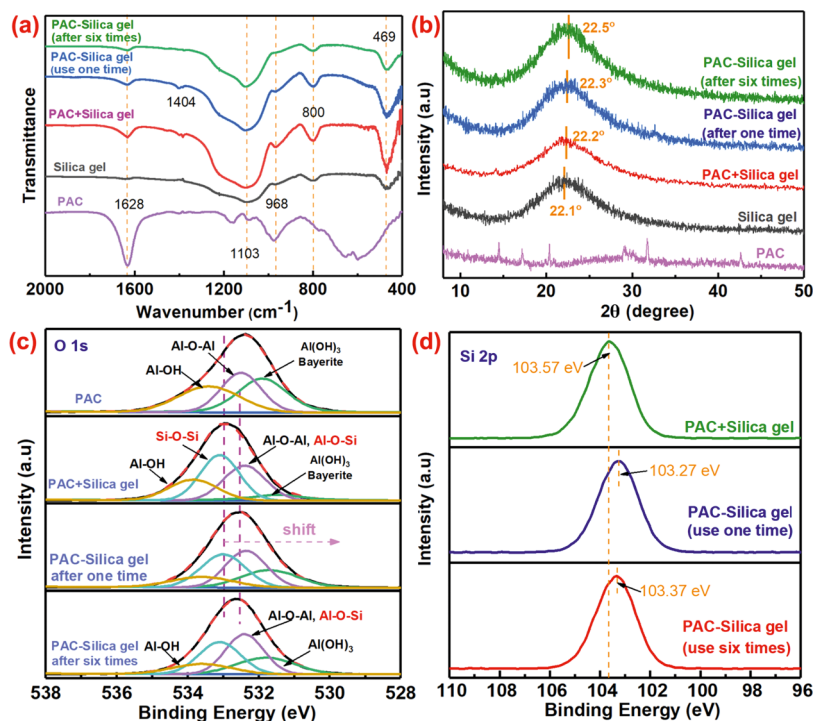


**Figure 4.** Structural information of the PAC–silica gel catalyst: (a) IR and (b) XRD. (c, d) The XPS spectra of O 1s and Si 2p.

force. This catalytic center is the essential factor for the high catalytic activity of the PAC–silica gel composite system.

**3.2. In Situ Conversion Mechanism of the PAC–Silica Gel Catalyst during the Mechanical Grinding Process.** Generally, the essence of the catalytic reaction is related to the active sites in the catalyst. The catalysts are characterized at various phases in the usage process to expose the mechanism

of the catalyst in the PAC–silica gel mechanical grinding system. The SEM and HRTEM images of the fresh PAC material are shown in Figure 3a<sub>1</sub>–a<sub>4</sub>. It can be seen that the fresh PAC material is a sphere with a diameter of 20–50 μm, which is caused by the spray drying process used in the preparation process. There are a variety of lattice fringes with unequal spacing in the fresh PAC material, indicating that the

surface of the PAC material exposes many Al–O active sites, which are densely cross-linked.<sup>38</sup> Figure 3b<sub>1</sub>,b<sub>2</sub> shows the images of the sample after simple mechanical mixing of PAC and silica gel. It can be found that grinding changes the morphology of the PAC material, destroying the original spherical structure and transforming it into a granular block when combined with silica gel. At this point, mechanical grinding is simply used to ensure uniform mixing; therefore, numerous lattice fringes with irregular spacing may still be visible in the HRTEM. An electronic picture of the catalyst after it has been employed once in the process is shown in Figure 3c<sub>1</sub>,c<sub>2</sub>. When the catalyst participates in the reaction, the catalyst particle size decreases and becomes more uniform, and the formerly brilliant lattice fringes vanish (Figure 3c<sub>4</sub>), transforming the state into a cross-linked state. Therefore, PAC and silica gel have changed during the reaction process. Because a very small amount of water can be produced during the reaction, a small amount of water and PAC and silica gel undergo chemical modifications under the action of mechanical grinding, establishing a new chemical bond (Al–O–Si bond). The same result is more obvious in the catalyst after six uses (Figure 3d<sub>1</sub>,d<sub>2</sub>). At this time, PAC and silica gel continuously react during multiple grinding and use, and the newly formed active sites are more and more uniformly dispersed in the entire catalyst system. PAC and silica gel are mixed to create a PAC–silica gel composite material at this moment. This is further validated by an energy spectrum scan of the PAC–silica gel substance. The three elements Al, O, and Si are uniformly distributed on the material's surface (Figure 3e–g).

To more accurately analyze the changes that occur during the reaction between PAC and silica gel, infrared, X-ray diffraction (XRD), and XPS were utilized to investigate the valence bond structure of the catalyst. Figure 4a displays the catalyst's infrared spectra in the 400–2000 cm<sup>-1</sup> region before and after usage. The O–H bending vibration absorption peak at 1629 cm<sup>-1</sup> in the infrared image indicates that the surface of the PAC–silica gel material has a substantial amount of hydroxyl groups.<sup>39</sup> This type of hydroxyl group is mainly derived from the Al–OH structure in the PAC material. During repeated usage, the peak at this location diminished, showing that the Al–OH structure was partially transformed. The peak at 1404 cm<sup>-1</sup> is considered to be the absorption peak of Ca–O tensile vibration, and a very small amount of Ca is introduced when adjusting the basicity during the preparation of PAC materials.<sup>40</sup> This result is likewise validated across the entire XPS element spectrum (Figure S1). After six times of use, the Ca–O absorption peak of the PAC–silica gel material diminishes or vanishes. This is because the PAC of the PAC–silica gel material changes during the grinding and use process, and the coordination effect of a small amount of Ca in the original structure is weakened. The peak at 1103 cm<sup>-1</sup> is attributed to the asymmetric tensile vibration absorption peaks of Si–O–Si and Al–O–Si bonds. Obviously, when PAC and silica gel are mixed and ground, the peak area of 1103 cm<sup>-1</sup> is larger than the area before grinding. This is because after adding PAC, mechanical stress causes PAC and silica gel to form new Al–O–Si bonds and the superposition of Al–O–Si and Si–O–Si bonds increases the peak area. In addition, the peaks at 968, 800, and 469 cm<sup>-1</sup> are all attributed to the characteristic absorption peaks of the Si–O bond. As the catalyst is used multiple times, the strength of the Si–O bond gradually weakens. This is because Al<sup>3+</sup> ions have an

isomorphous substitution of Si<sup>4+</sup> in silica gel, and part of the Si–O–Si bonds are transformed to form Al–O–Si bonds. In addition, the recent research results show that with high yields, intramolecular reactions are important for gels.<sup>41</sup> The silicone material reported in this work can be considered as a special kind of gel with silicon as the main element. The Si–O–Si bonds within the silica molecule and the Al–O–Al bonds in the PAC material undergo intramolecular reactions mentioned in the above literature under the action of mechanical forces, which continuously recombine and reorganize to finally form Al–O–Si bonds. Figure 4b is the XRD pattern of the material. Both PAC and silica gel show amorphous broad peaks.<sup>42</sup> The new composite material obtained after grinding mainly shows the amorphous broad peaks of silica gel. It can be found that the score center of the peak at 22° is slightly shifted from 22.1 to 22.5°. This once again confirmed that PAC and silica gel combined to form a new Al–O–Si bond during the grinding process.

The formation and transformation process of the PAC–silica gel composite catalyst was elucidated from the microscopic electronic structure by XPS test analysis. The energy spectrum of O 1s in the material was fitted to the split peaks using a Gaussian function, and the results are shown in Figure 4c. The O element in PAC can be fitted to three coordination structures with peak centers at 531.9, 532.5, and 533.4 eV, representing Ca-containing Al(OH)<sub>3</sub>, Al–O–Al, and Al–OH, respectively.<sup>43,44</sup> When PAC and silica gel were ground together, the peaks of O 1s were shifted to the high binding energy direction as a whole, which was caused by the enhancement of the peaks of Si–O–Si bonds in the catalytic system with the addition of silica gel.<sup>45</sup> It can also be found that the peak area of the original Al–O–Al bond in the material increases significantly after mixing and grinding. This is due to the formation of a new Al–O–Si bond between PAC and silica gel at 532.4 eV during the grinding process, and the presence of both Al–O–Si and Al–O–Al bonds enhances the peak area here. The overall shift of the O 1s peak toward lower binding energy after putting the composite into the reaction for one use is due to the adsorption of Al<sup>3+</sup> cations by Si during grinding and use, which increases the electron cloud density around the O atom and shields the O atom.<sup>46</sup> A further enhancement of the peak area at 532.4 eV can also be found, which is due to the fact that two molecules of water are shed during the reaction when involved, and the presence of water promotes the formation of Al–O–Si bonds between PAC and silica gel. The amount of Al–O–Si bonds formed by trace water in the environment alone during grinding was less than that generated directly during the reaction compared to the material before the reaction is engaged. In addition, a gradual weakening of the peak of the Al–OH bond can be found during multiple applications, which again verifies the shift from the initial hydroxyl coordination to Si coordination around Al. An increase in the peak area at 531.9 eV was found in the material used six times repeatedly, and this peak was attributed to the peak of Al(OH)<sub>3</sub> generated during the grinding process. This indicates that a portion of Al is converted to Al(OH)<sub>3</sub> during this recycling process. Because of the low catalytic activity of Al(OH)<sub>3</sub>, the PAC–silica composite catalyst takes a longer time to complete the reaction during recycling. Figure 4d shows the spectrum of Si 2p of the material before and after grinding, and it can be found that the peak center of Si shifts toward the lower binding energy after grinding.<sup>47</sup> This is due to the introduction of the metal cation Al, which promotes the

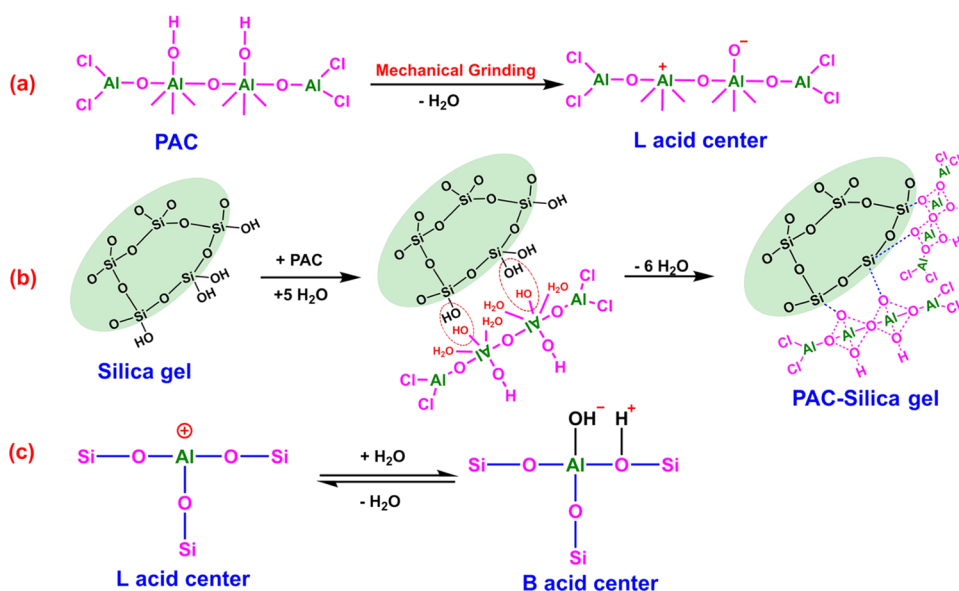


**Figure 5.** Formation of the Al–O–Si catalytic active center under in situ grinding conditions: (a) the structure of PAC materials; (b) the structure of PAC–silica gel materials; and (c) the structure of the Al–O–Si catalytic active center.

bonding of Al and Si in the form of an oxygen bridge by mechanical forces, and the newly formed Al–O–Si bond shifts the peak center of Si.

The process of PAC and silica gel in the formation of new catalytic activity during the grinding process is shown in Figure 5. The Al elements in PAC materials are connected together by Al–O bridges, which undergo changes as shown in Figure 5a when mechanically ground, exhibiting L acid centers, which is one of the reasons why PAC materials can be used as L acids to catalyze organic synthesis reactions.<sup>48</sup> When PAC is mechanically ground together with silica gel, PAC will adsorb water from the environment to form hydrated hydroxy aluminum, which condenses with the hydroxyl groups on the surface of silica gel particles to form silica gel–PAC complexes (Figure 5b).<sup>49</sup> Because the amount of silica gel is much larger than the amount of aluminum elements in PAC and the reaction property of silica gel is stronger, this local reaction occurs continuously and many times under the grinding action. The structure of Al–O–Si will be more than the structure of Al–O–Al in the material after a long time of grinding, and finally, the aluminum atoms will form the structure, as shown in Figure 5c. The formation of Al–O–Si bonds is the essential reason for the higher catalytic activity of the PAC–silica composite catalyst. On the surface of the silica gel–PAC complex, each aluminum ion is surrounded by three silicon atoms (via oxygen bridging), but one coordination silicon toward the outer surface direction is missing (Figure 5c). This asymmetric distribution of silicon atoms leads to an extremely strong electrophile property of the aluminum ion. When the environment or the water produced by the reaction is close to this aluminum ion, the negatively charged hydroxyl group of the water molecule is attracted to the aluminum ion, separating a proton to form a B acid, and the original triple-ligated aluminum acts as an L acid. In other words, it is the homocrystalline substitution of Al<sup>3+</sup> ions for Si<sup>4+</sup> ions in the silica gel skeleton that causes an excess negative charge at the substitution site, so H<sup>+</sup> that plays a role in leveling the electrical properties becomes a B acid center.<sup>50</sup> If the acidic hydroxyl group is removed by heat in the form of water to

form triple-ligated aluminum, it is transformed into an L acid center. The B acid and L acid centers can be interconverted during the catalytic reaction, exhibiting synergistic catalysis.

In addition, PAC, silica gel, and PAC–silica gel materials were tested using NH<sub>3</sub>-TPD, and the results are shown in Figure 6. The PAC material alone has poor thermal stability,

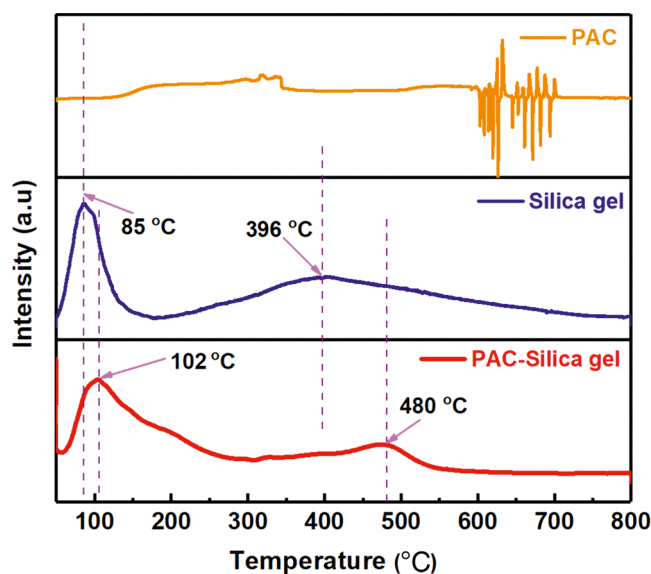


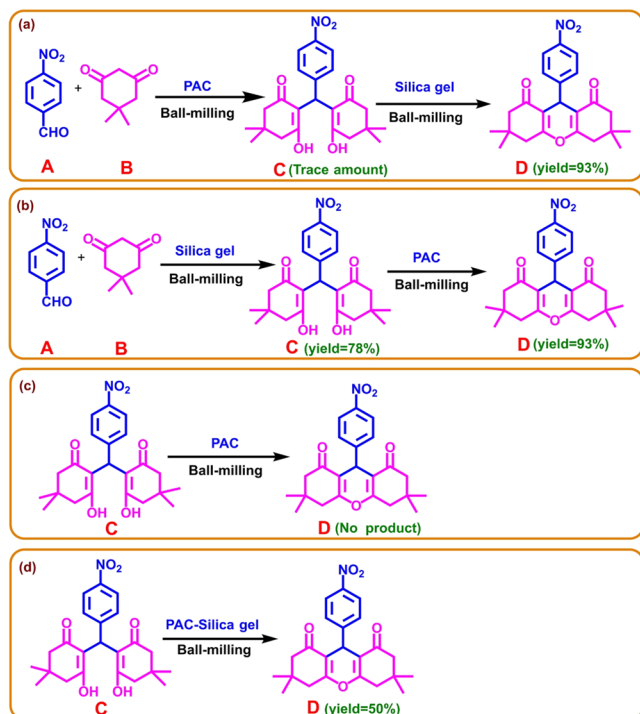
**Figure 6.** NH<sub>3</sub>-TPD of PAC, silica gel, and PAC–silica gel materials.

and the material melts and decomposes above 600°. The complete NH<sub>3</sub>-TPD curve was not obtained because of the variation in its structural properties. The silica gel material shows two absorption peaks at 85 and 396 °C, with the absorption peak at the lower temperature being sharper and of high relative intensity, indicating that the silica gel material is less acidic. This acidic site probably originates from the Si–OH structure on the surface of silica gel. The PAC–silica gel composite shows absorption peaks at 50–300 and 400–550 °C, indicating that the PAC–silica gel material has two acidic

adsorption sites of different intensities. Compared to the PAC material alone, the composite has enhanced thermal stability and remains stable in the high-temperature region. The absorption peaks of PAC–silica gel composites appear at higher temperatures than silica alone. Usually, the higher the temperature at which the adsorption peak of the acidic adsorption site appears, the more acidic the material is. This change in performance in the  $\text{NH}_3$ -TPD test after the reaction of PAC with silica gel grinding may be due to mechanical ball milling inducing the formation of new Al–O–Si bonds by combining PAC with silica gel.

**3.3. Investigation of the Mechanism of the PAC–Silica Gel Catalyst-Catalyzed Xanthene Reaction.** The role of PAC and silica gel in the catalytic process was analyzed in detail using the synthesis of xanthene compounds as a typical case (Scheme 3). The step-by-step control of the

**Scheme 3. Role of PAC, Silica Gel, and PAC–Silica Gel in Catalyzing the Synthesis of 1,8-Dioxo-octahydroanthracene Compounds<sup>a</sup>**



<sup>a</sup>(a) Adding PAC first; (b) adding silica gel first; (c) catalyzed with PAC; and (d) catalyzed with PAC–silica gel.

reaction process was achieved by changing the catalyst addition method to gradually add PAC and silica gel in batches. It was found that intermediate compound C is produced during the reaction, and PAC basically does not prompt the reaction (Scheme 3a), but silica alone gives compound C in 78% yield. End product D is not produced unless the PAC material is continued to be added to the process (Scheme 3b). This indicates that silica gel plays a critical role in facilitating the first stage of the catalytic process. PAC alone cannot complete the second stage of the reaction (Scheme 3c), and it is necessary to grind PAC together with silica gel for the reaction to work. In other words, the Al–O–Si active species produced by the compounding of PAC with silica gel is the real catalytic center of the second stage. Because of the lack of water

promotion, PAC and silica gel do not immediately form Al–O–Si active species, so only 50% of the products are generated during the transition from C to D molecules (Scheme 3d).

The development of density functional theory has provided more options for the interpretation of mechanisms in chemistry, especially in organic chemistry. This is the first time we report the use of silica–PAC composite catalysts for the catalytic synthesis of xanthene. By calculating the energy required in the reaction path for different catalyst cases, the phenomenon in Scheme 3 can be revealed more clearly. Although the polymeric aluminum chloride materials are complex inorganic polymers with multiple structures of Al–O cationic nuclei, their dominant unit structure is the Al–O–Al structure. Therefore,  $\text{Al}_3\text{O}_2$  with a similar structure is used in modeling to represent complex polymeric aluminum chloride.<sup>51</sup> The calculated results of the catalytic path are shown in Figure 7. Figure 7a shows the simulation results when the Al–O–Al structure is the catalytic active site, and the process of slab-d generation from slab-c is its limiting link, which requires a critical energy barrier of 5.97 eV. Figure 7b shows the simulation results with silica gel (Si–O–Si) as the active site. The process of slab-b generation from slab-a is the limiting link of Si–O–Si catalysis, and the energy required to complete the reaction is 6.24 eV. However, when polymeric aluminum chloride and silica gel are ground together, they are compounded by mechanical forces to reconstitute the new catalytically active center, the Al–O–Si bond. At this point, the formation of slab-b from slab-a is the limiting link catalyzed by Al–O–Si, and the energy required to complete the reaction is 4.38 eV (Figure 7c). It is clear that the PAC–silica composite catalyst (Al–O–Si, 4.38 eV) requires much less energy than the PAC material (Al–O–Al, 6.24 eV) and also much lower than the silica material (Si–O–Si, 5.97 eV). This proves that the new catalytic active site (Al–O–Si) constituted by mechanical grinding is the real reason for the rapid occurrence of the reaction. Observing the bonding state of molecules in the key reaction step of Al–O–Si active sites during catalysis (Figure 7d), it can be found that the reacting molecules will first interact with Al sites in the composite and then gradually transform to interact with both Al and Si sites. This change process also reflects the important role of the Al–O–Si bond formed by mechanical grinding in the catalytic reaction process.

Based on the above findings, we proposed a possible mechanism for the PAC–silica gel system in catalyzing the reaction of aldehydes with cyclohexanedione (Figure 8). First, one molecule of dimethylcyclohexanedione is activated by the hydroxyl group on the surface of silica gel to produce compound (2). A molecule of aldehyde, also activated by the hydroxyl group on the silica surface, was added to compound (2) by the Knoevenagel reaction to produce compound (3). Compound (3) loses one molecule of water in the presence of grinding and heat to form compound (4). At this point, another molecule of activated dimethyl ketone is reacted with compound (4) to produce compound (5) by the Michael addition reaction. Compound (5) undergoes reciprocal isomerization to form intermediate compound (6). Compound (6) formed the target product by in-ring dehydration through coordination with the active center Al–O–Si produced by in situ mechanical grinding in the PAC–silica gel system. During the whole reaction process, silica gel is used as a cocatalyst to assist in the completion of the previous stage of the reaction, and the Al–O–Si produced in situ by PAC and silica gel

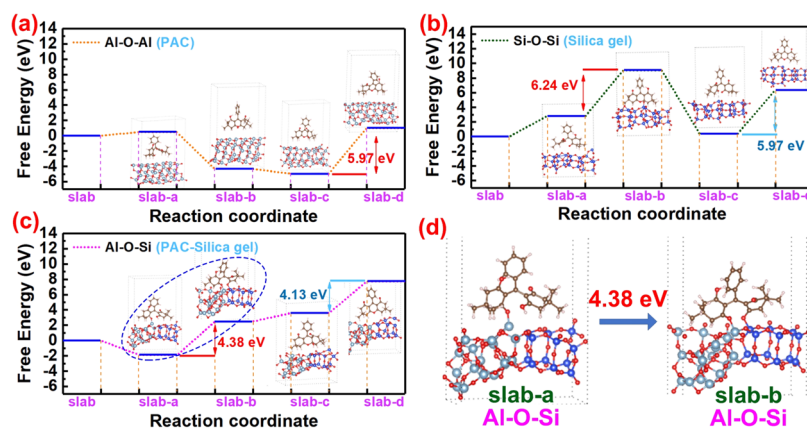


**Figure 7.** Density functional theory during the synthesis of xanthenes compounds: (a) catalyzed with PAC; (b) catalyzed with silica gel; and (c) catalyzed with PAC–silica gel. (d) Schematic diagram of slab-a to slab-b in the PAC–silica gel catalytic process.

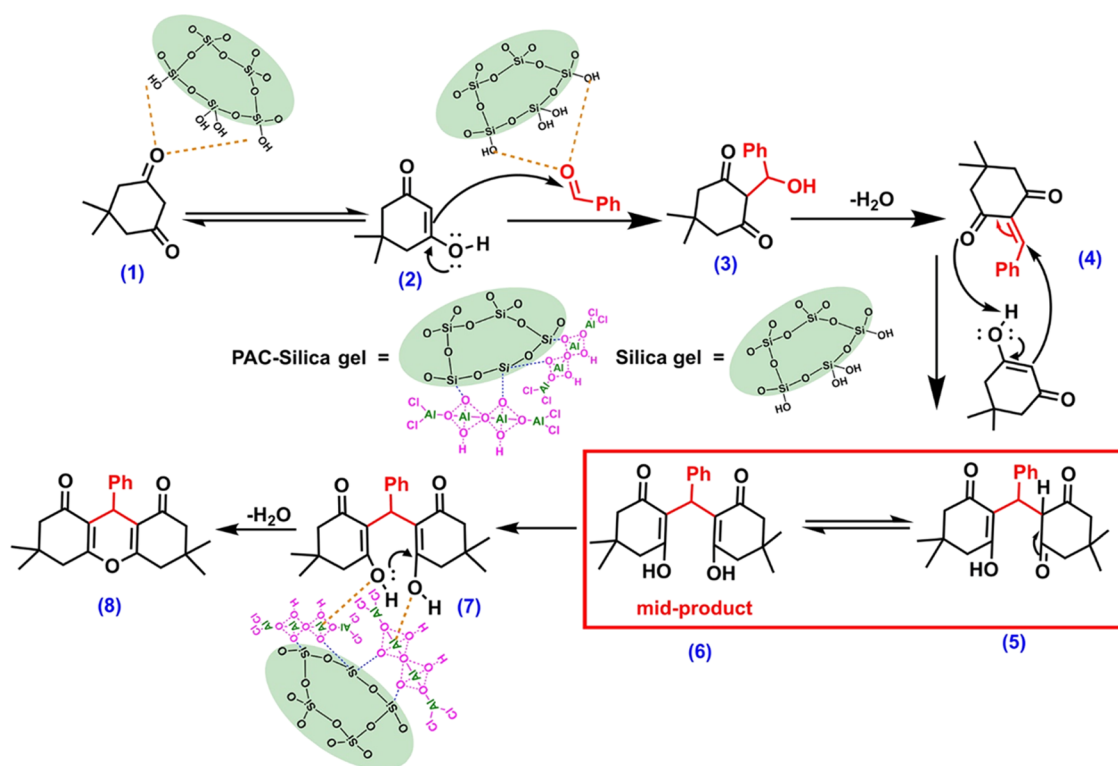


**Figure 8.** Possible mechanism for the synthesis of 1,8-dioxo-octahydroanthracene compounds by PAC–silica gel catalysts.

during the mechanical grinding process is the key to the completion of the reaction. In addition, by comparing the PAC–silica composite catalyst system with other literature of the same type (Table 1), it can be found that the PAC–silica composite catalyst has the advantages of being green and inexpensive and having high stability. The in situ transformation of active sites under mechanical grinding conditions provides unlimited possibilities for its wider application in green synthesis and catalysis.

#### 4. CONCLUSIONS

In summary, we report a new method for the synthesis of xanthenes and pyrimidinone compounds using mechanical ball milling assistance. In this process, the compounds and catalytic materials (aluminum chloride and silica gel) are added directly by the “one-pot” method. Mechanical ball milling serves two

purposes: first, it allows silica gel and PAC to be assembled into a composite material, and second, it acts as a driving force for the catalytic reaction to take place. From a practical application point of view, this one-pot method of catalysis eliminates the complex preparation process of catalyst materials. The PAC–silica gel catalyst has high stability and wide applicability, and the material is widely available and inexpensive. Taking the synthesis of 1,8-dioxo-octahydroanthracene compounds as an example, the mechanism of action of in situ complexation of polymeric aluminum chloride with silica gel was revealed through the characterization analysis of the catalyst before and after use. The results show that polymerized aluminum chloride and silica gel were compounded and reconstituted under the action of mechanical grinding to generate the PAC–silica gel composite catalytic system (Al–O–Si active center) in situ. The silica gel plays the

**Table 1. Different Types of Catalysts for the Synthesis of 2,2'-Aryl-methylenebis(3-hydroxy-2-cyclohexene-1-one) Derivatives**

entry	reaction condition	reuse (times)	refs
1	PANI-PTSI, 25 wt %, water reflux, 6 h, 84%	6	52
2	PPA-SiO <sub>2</sub> , 10 mol %, solvent-free, 140 °C, 0.5 h, 71%		37
3	glycerol, 2.0 g, solvent-free, 90 °C, 2.5 h, 94%		36
4	SbCl <sub>3</sub> /SiO <sub>2</sub> , 10 mmol %, solvent-free, 120 °C, 45 min, 94%	3	53
5	Al(DS) <sub>3</sub> , 20 mol %, solvent-free, 80 °C, 10 min, 80%	5	54
6	SD-OS <sub>3</sub> H, 0.0061 mmol, EtOH reflux, 35 min, 90%	3	32
7	FeNp@SBA-15, 0.5 mol %, solvent-free, 80 °C, 20 min, 99%	12	31
8	ZNPS, 10 mol %, deionized water, 60–70 °C, 90 min, 60%		34
9	BAILS, 10 mol %, solvent-free, 100 °C, 45 min, 95%	5	33
10	ZrOCl <sub>2</sub> ·8H <sub>2</sub> O, 2 mol %, solvent-free, 85 °C, 30 min, 87%		30
11	PAC-silica gel, 0.018 mol %, solvent-free, ball milling, 24 min, 92%	6	this work

role of a cocatalyst. Finally, the energy barriers that need to be crossed by different catalysts in the reaction were calculated using density flooding theory, and the PAC-silica composite system requires the lowest energy, so the composite system (PAC-silica) is the real catalytic activity center. The research in this paper is a successful example of the application of mechanochemistry in materials and organic synthesis, offering unlimited possibilities for the application of inorganic polymer materials in green synthesis and catalysis promoted by mechanochemistry.

## ■ ASSOCIATED CONTENT

### SI Supporting Information

The Supporting Information is available free of charge at <https://pubs.acs.org/doi/10.1021/acsomega.2c04159>.

Optimization of conditions for the synthesis reaction of catalytic xanthene compounds (Table S1); reuse of catalysts (Table S2); synthesis of xanthene with different substituent groups (Table S3); full spectrum of the XPS test of PAC-silica gel catalysts (Figure S1); reaction paths of different catalysts (Figure S2); and data and spectra of products (Figures S3–S46) (PDF)

## ■ AUTHOR INFORMATION

### Corresponding Authors

**Haijuan Zhan** – State Key Laboratory of High-Efficiency Utilization of Coal and Green Chemical Engineering, National Demonstration Center for Experimental Chemistry Education, College of Chemistry and Chemical Engineering, Ningxia University, Yinchuan 750021, P. R. China; Email: [drzhj1225@126.com](mailto:drzhj1225@126.com)

**Wanyi Liu** – State Key Laboratory of High-Efficiency Utilization of Coal and Green Chemical Engineering, National Demonstration Center for Experimental Chemistry Education, College of Chemistry and Chemical Engineering, Ningxia University, Yinchuan 750021, P. R. China; [orcid.org/0000-0003-1059-6437](https://orcid.org/0000-0003-1059-6437); Email: [liuwuy@nxu.edu.cn](mailto:liuwuy@nxu.edu.cn)

## Authors

**Gang Wang** – State Key Laboratory of High-Efficiency Utilization of Coal and Green Chemical Engineering, National Demonstration Center for Experimental Chemistry Education, College of Chemistry and Chemical Engineering, Ningxia University, Yinchuan 750021, P. R. China

**Yage Geng** – State Key Laboratory of High-Efficiency Utilization of Coal and Green Chemical Engineering, National Demonstration Center for Experimental Chemistry Education, College of Chemistry and Chemical Engineering, Ningxia University, Yinchuan 750021, P. R. China

**Zejing Zhao** – State Key Laboratory of High-Efficiency Utilization of Coal and Green Chemical Engineering, National Demonstration Center for Experimental Chemistry Education, College of Chemistry and Chemical Engineering, Ningxia University, Yinchuan 750021, P. R. China

**Qiuping Zhang** – State Key Laboratory of High-Efficiency Utilization of Coal and Green Chemical Engineering, National Demonstration Center for Experimental Chemistry Education, College of Chemistry and Chemical Engineering, Ningxia University, Yinchuan 750021, P. R. China

**Xiang Li** – State Key Laboratory of High-Efficiency Utilization of Coal and Green Chemical Engineering, National Demonstration Center for Experimental Chemistry Education, College of Chemistry and Chemical Engineering, Ningxia University, Yinchuan 750021, P. R. China

**Zhiqiang Wu** – College of Chemistry and Chemical Engineering, Ningxia Normal University, Guyuan 756000, P. R. China

**Shuxian Bi** – State Key Laboratory of High-Efficiency Utilization of Coal and Green Chemical Engineering, National Demonstration Center for Experimental Chemistry Education, College of Chemistry and Chemical Engineering, Ningxia University, Yinchuan 750021, P. R. China

Complete contact information is available at:

<https://pubs.acs.org/10.1021/acsomega.2c04159>

## Notes

The authors declare no competing financial interest.

## ■ ACKNOWLEDGMENTS

This work was financially supported by the National Natural Science Foundation of China (No. 22162021), the Natural Science Foundation of Ningxia Province (No. 2021AAC03057), and the 2022 Autonomous Region Key R&D Program General Project (No. 2022BDE03013).

## ■ REFERENCES

- Escher, B. I.; Stapleton, H. M.; Schymanski, E. L. Tracking complex mixtures of chemicals in our changing environment. *Science* **2020**, *367*, 388–392.
- Hessel, V.; Tran, N. N.; Asrami, M. R.; Tran, Q. D.; van Duc Long, N.; Escribà-Gelonch, M.; Tejada, J. O.; Linke, S.; Sundmacher, K. Sustainability of green solvents – review and perspective. *Green Chem.* **2022**, *24*, 410–437.
- Kol, R.; De Somer, T.; D'Hooge, D. R.; Knappich, F.; Ragaert, K.; Achillas, D. S.; De Meester, S. State-Of-The-Art Quantification of Polymer Solution Viscosity for Plastic Waste Recycling. *ChemSusChem* **2021**, *14*, 4071–4102.
- Clarke, C. J.; Tu, W. C.; Levers, O.; Brohl, A.; Hallett, J. P. Green and Sustainable Solvents in Chemical Processes. *Chem. Rev.* **2018**, *118*, 747–800.

- (5) Amrute, A. P.; De Bellis, J.; Felderhoff, M.; Schuth, F. Mechanochemical Synthesis of Catalytic Materials. *Chem. - Eur. J.* **2021**, *27*, 6819–6847.
- (6) Wang, L.; Xin, B.; Elskova, A.; Eklund, P.; Solin, N. Mechanochemical Formation of Protein Nanofibril: Graphene Nanoplatelet Hybrids and Their Thermoelectric Properties. *ACS Sustainable Chem. Eng.* **2020**, *8*, 17368–17378.
- (7) Friščić, T.; Mottillo, C.; Titi, H. M. Mechanochemistry for Synthesis. *Angew. Chem.* **2020**, *132*, 1030–1041.
- (8) Howard, J. L.; Cao, Q.; Browne, D. L. Mechanochemistry as an emerging tool for molecular synthesis: what can it offer. *Chem. Sci.* **2018**, *9*, 3080–3094.
- (9) Wilke, M.; Casati, N. A new route to polyoxometalates via mechanochemistry. *Chem. Sci.* **2022**, *13*, 1146–1151.
- (10) Seo, T.; Ishiyama, T.; Kubota, K.; Ito, H. Solid-state Suzuki-Miyaura cross-coupling reactions: olefin-accelerated C-C coupling using mechanochemistry. *Chem. Sci.* **2019**, *10*, 8202–8210.
- (11) Kubota, K.; Takahashi, R.; Ito, H. Mechanochemistry allows carrying out sensitive organometallic reactions in air: glove-box-and-Schlenk-line-free synthesis of oxidative addition complexes from aryl halides and palladium(0). *Chem. Sci.* **2019**, *10*, 5837–5842.
- (12) Ralphs, K.; D'Agostino, C.; Burch, R.; Chansai, S.; Gladden, L. F.; Hardacre, C.; James, S. L.; Mitchell, J.; Taylor, S. F. R. Assessing the surface modifications following the mechanochemical preparation of a Ag/Al<sub>2</sub>O<sub>3</sub> selective catalytic reduction catalyst. *Catal. Sci. Technol.* **2014**, *4*, 531–539.
- (13) Ardila-Fierro, K. J.; Hernandez, J. G. Sustainability Assessment of Mechanochemistry by Using the Twelve Principles of Green Chemistry. *ChemSusChem* **2021**, *14*, 2145–2162.
- (14) Zappimulso, N.; Capozzi, M. A. M.; Porcheddu, A.; Farinola, G. M.; Punzi, A. Solvent-free Reactions for the Synthesis of Indolenine-based Squaraines and Croconaines: Comparison of Thermal Heating, Mechanochemical Milling, and IR Irradiation. *ChemSusChem* **2021**, *14*, 1363–1369.
- (15) Piquero, M.; Font, C.; Gullon, N.; Lopez-Alvarado, P.; Menendez, J. C. One-Pot Mechanochemical Synthesis of Mono- and Bis-Indolylquinones via Solvent-Free Multiple Bond-Forming Processes. *ChemSusChem* **2021**, *14*, 4764–4775.
- (16) Dayaker, G.; Tan, D.; Biggins, N.; Shelam, A.; Do, J. L.; Katsenis, A. D.; Friscic, T. Catalytic Room-Temperature C-N Coupling of Amides and Isocyanates by Using Mechanochemistry. *ChemSusChem* **2020**, *13*, 2966–2972.
- (17) Guo, J.; Zhou, Z.; Ming, Q.; Huang, Z.; Zhu, J.; Zhang, S.; Xu, J.; Xi, J.; Zhao, Q.; Zhao, X. Recovering precipitates from dechlorination process of saline wastewater as poly aluminum chloride. *Chem. Eng. J.* **2022**, *427*, No. 131612.
- (18) Matsui, Y.; Shirasaki, N.; Yamaguchi, T.; Kondo, K.; Machida, K.; Fukuura, T.; Matsushita, T. Characteristics and components of poly-aluminum chloride coagulants that enhance arsenate removal by coagulation: Detailed analysis of aluminum species. *Water Res.* **2017**, *118*, 177–186.
- (19) Yan, M.; Wang, D.; Qu, J.; He, W.; Chow, C. W. Relative importance of hydrolyzed Al(III) species (Al(a), Al(b), and Al(c)) during coagulation with polyaluminum chloride: a case study with the typical micro-polluted source waters. *J. Colloid Interface Sci.* **2007**, *316*, 482–489.
- (20) Ni, F.; He, J.; Wang, Y.; Luan, Z. Preparation and characterization of a cost-effective red mud/polyaluminum chloride composite coagulant for enhanced phosphate removal from aqueous solutions. *J. Water Process Eng.* **2015**, *6*, 158–165.
- (21) Wang, G.; Hao, P.; Liang, Y.; Liang, Y.; Liu, W.; Wen, J.; Li, X.; Zhan, H.; Bi, S. The new life of traditional water treatment flocculant polyaluminum chloride (PAC): a green and efficient micro-nano reactor catalyst in alcohol solvents. *RSC Adv.* **2021**, *12*, 655–663.
- (22) Liang, Y.; Wang, G.; Wu, Z.; Liu, W.; Song, M.; Sun, Y.; Chen, X.; Zhan, H.; Bi, S. "Inorganic Polymer Flocculation Catalyst"—Polyaluminum chloride as highly efficient and green catalyst for the Friedel-Crafts alkylation of bis(indolyl)methanes. *Catal. Commun.* **2020**, *147*, No. 106136.
- (23) Alzeer, M. I. M.; MacKenzie, K. J. D. Synthesis and Catalytic Properties of New Sustainable Aluminosilicate Heterogeneous Catalysts Derived from Fly Ash. *ACS Sustainable Chem. Eng.* **2018**, *6*, 5273–5282.
- (24) Lu, M.; Fatah, N.; Khodakov, A. Y. New shearing mechanical coating technology for synthesis of alumina-supported cobalt Fischer-Tropsch solid catalysts. *J. Mater. Chem. A* **2017**, *5*, 9148–9155.
- (25) Pichaikaran, S.; Arumugam, P. Vapour phase hydrodeoxygenation of anisole over ruthenium and nickel supported mesoporous aluminosilicate. *Green Chem.* **2016**, *18*, 2888–2899.
- (26) Zhang, Y.; Ye, S.; Gao, M.; Li, Y.; Huang, X.; Song, J.; Cai, H.; Zhang, Q.; Zhang, J. N-Doped Graphene Supported Cu Single Atoms: Highly Efficient Recyclable Catalyst for Enhanced C–N Coupling Reactions. *ACS Nano* **2022**, *16*, 1142–1149.
- (27) Verma, P.; Truhlar, D. G. Status and Challenges of Density Functional Theory. *Trends Chem.* **2020**, *2*, 302–318.
- (28) Li, C.; Wang, G.; Li, K.; Liu, Y.; Yuan, B.; Lin, Y. FeNi-Based Coordination Crystal Directly Serving as Efficient Oxygen Evolution Reaction Catalyst and Its Density Functional Theory Insight on the Active Site Change Mechanism. *ACS Appl. Mater. Interfaces* **2019**, *11*, 20778–20787.
- (29) Pladevall, B. S.; de Aguirre, A.; Maseras, F. Understanding Ball Milling Mechanochemical Processes with DFT Calculations and Microkinetic Modeling. *ChemSusChem* **2021**, *14*, 2763–2768.
- (30) Menezes, A. P. D. J.; Silva, M. L. D.; Pereira, W. L.; Costa, G. P.; Horta, A. L.; Mendonca, A. A. S.; Carneiro, A. C. A.; Souza, D. M. S.; Novaes, R. D.; Teixeira, R. R.; Talvani, A. In vitro tripanocidal effect of 1,8-dioxooctahydroxanthenes (xanthenodiones) and tetraketones and improvement of cardiac parameters in vivo. *J. Global Antimicrob. Resist.* **2020**, *22*, 466–476.
- (31) Rajabi, F.; Abdollahi, M.; Diarjani, E. S.; Osmolowsky, M. G.; Osmolovskaya, O. M.; Gomez-Lopez, P.; Puente-Santiago, A. R.; Luque, R. Solvent-Free Preparation of 1,8-Dioxo-Octahydroxanthenes Employing Iron Oxide Nanomaterials. *Materials* **2019**, *12*, No. 2386.
- (32) NaiduKalla, R. M.; Karunakaran, R. S.; Balaji, M.; Kim, I. Catalyst-Free Synthesis of Xanthene and Pyrimidine-Fused Heterocyclic Derivatives at Water-Ethanol Medium and Their Antioxidant Properties. *ChemistrySelect* **2019**, *4*, 644–649.
- (33) Ashtarian, J.; Heydari, R.; Maghsoodlou, M.-T.; Yazdani-Elah-Abadi, A. Bronsted Acidic Ionic Liquids (BAILs)-Catalyzed Synthesis of 1,8-Dioxo-Octahydroxanthene and 2,2'-Arylmethylene Bis(3-Hydroxy-5,5-Dimethyl-2-Cyclohexene-1-One) Derivatives Under Eco-Friendly Conditions. *Iran. J. Sci. Technol., Trans. A: Sci.* **2020**, *44*, 51–64.
- (34) Abdelghany, A. M.; Menazea, A. A.; Abd-El-Maksoud, M. A.; Khatab, T. K. Pulsed laser ablated zeolite nanoparticles: A novel nano-catalyst for the synthesis of 1,8-dioxo-octahydroxanthene and N-aryl-1,8-dioxodecahydroacridine with molecular docking validation. *Appl. Organomet. Chem.* **2019**, *34*, No. e5250.
- (35) Kazemi-Rad, R.; Azizian, J.; Kefayati, H. Improved Synthesis of 2,2-Arylmethylene Bis(3-hydroxy-5,5-dimethyl-2-cyclohexene-1-one) and 1,8-Dioxo-octahydroxanthene Derivatives Catalyzed by Electro-generated Base and Sulfuric Acid. *J. Chin. Chem. Soc.* **2015**, *62*, 311–315.
- (36) Zhang, Z.-H.; Liu, Y.-H. Antimony trichloride/SiO<sub>2</sub> promoted synthesis of 9-ary-3,4,5,6,7,9-hexahydroxanthene-1,8-diones. *Catal. Commun.* **2008**, *9*, 1715–1719.
- (37) Kantevari, S.; Bantu, R.; Nagarapu, L. HClO<sub>4</sub>–SiO<sub>2</sub> and PPA–SiO<sub>2</sub> catalyzed efficient one-pot Knoevenagel condensation, Michael addition and cyclo-dehydration of dimedone and aldehydes in acetonitrile, aqueous and solvent free conditions: Scope and limitations. *J. Mol. Catal. A: Chem.* **2007**, *269*, 53–57.
- (38) Casey, W. H. Large aqueous aluminum hydroxide molecules. *Chem. Rev.* **2006**, *106*, 1–16.
- (39) Hameed, Y. T.; Idris, A.; Hussain, S. A.; Abdullah, N. A tannin-based agent for coagulation and flocculation of municipal wastewater: Chemical composition, performance assessment compared to

Polyaluminum chloride, and application in a pilot plant. *J. Environ. Manage.* **2016**, *184*, 494–503.

(40) Tang, H.; Xiao, F.; Wang, D. Speciation, stability, and coagulation mechanisms of hydroxyl aluminum clusters formed by PACl and alum: A critical review. *Adv. Colloid Interface Sci.* **2015**, *226*, 78–85.

(41) De Keer, L.; Kilic, K. I.; Van Steenberge, P. H. M.; Daelemans, L.; Kodura, D.; Frisch, H.; De Clerck, K.; Reyniers, M. F.; Barner-Kowollik, C.; Dauskardt, R. H.; D'Hooge, D. R. Computational prediction of the molecular configuration of three-dimensional network polymers. *Nat. Mater.* **2021**, *20*, 1422–1430.

(42) Tang, X.; Zheng, H.; Teng, H.; Zhao, C.; Wang, Y.; Xie, W.; Chen, W.; Yang, C. An alternative method for preparation of polyaluminum chloride coagulant using fresh aluminum hydroxide gels: Characterization and coagulation performance. *Chem. Eng. Res. Des.* **2015**, *104*, 208–217.

(43) Musigapong, P.; Briffa, S. M.; Lynch, I.; Soontaranon, S.; Chanlek, N.; Valsami-Jones, E. In *Silica Nanoparticle Synthesis and Multi-Method Characterisation*, Materials Science Forum; Trans Tech Publications Ltd., 2019; Vol. 947, pp 82–90.

(44) Liang, L.; Tan, J.; Peng, Y.; Xia, W.; Xie, G. The role of polyaluminum chloride in kaolinite aggregation in the sequent coagulation and flocculation process. *J. Colloid Interface Sci.* **2016**, *468*, 57–61.

(45) Ma, H.; Jiao, K.; Xu, X.; Song, J. Synthesis and Characterization of a New Aluminosilicate Molecular Sieve from Aluminosilicate Perhydrate Hydrogel. *Materials* **2020**, *13*, No. 5469.

(46) Black, L.; Garbev, K.; Stemmermann, P.; Hallam, K. R.; Allen, G. C. X-ray photoelectron study of oxygen bonding in crystalline C-S-H phases. *Phys. Chem. Miner.* **2004**, *31*, 337–346.

(47) Moreno-Martínez, V. A.; Marti Nez-Otero, D.; Meza-Gonzalez, B.; Cortez-Guzman, F.; Jancik, V. Aluminum-Triggered Condensation of Vicinal Silicate Groups into a Bicyclic Aluminosilicate. *Inorg. Chem.* **2020**, *59*, 6849–6856.

(48) Wang, C.; Guo, H.; Leng, S.; Yu, J.; Feng, K.; Cao, L.; Huang, J. Regulation of hydrophilicity/hydrophobicity of aluminosilicate zeolites: a review. *Crit. Rev. Solid State Mater. Sci.* **2021**, *46*, 330–348.

(49) Nada, M. H.; Larsen, S. C.; Gillan, E. G. Mechanochemically-assisted solvent-free and template-free synthesis of zeolites ZSM-5 and mordenite. *Nanoscale Adv.* **2019**, *1*, 3918–3928.

(50) Herrmann, S.; Iglesia, E. Elementary steps in acetone condensation reactions catalyzed by aluminosilicates with diverse void structures. *J. Catal.* **2017**, *346*, 134–153.

(51) Chizallet, C. Toward the Atomic Scale Simulation of Intricate Acidic Aluminosilicate Catalysts. *ACS Catal.* **2020**, *10*, 5579–5601.

(52) John, A.; Yadav, P. J. P.; Palaniappan, S. Clean synthesis of 1,8-dioxo-dodecahydroxanthene derivatives catalyzed by polyaniline-p-toluenesulfonate salt in aqueous media. *J. Mol. Catal. A: Chem.* **2006**, *248*, 121–125.

(53) He, F.; Li, P.; Gu, Y.; Li, G. Glycerol as a promoting medium for electrophilic activation of aldehydes: catalyst-free synthesis of di(indolyl)methanes, xanthene-1,8(2H)-diones and 1-oxo-hexahydroxanthenes. *Green Chem.* **2009**, *11*, 1767–1773.

(54) Firouzabadi, H.; Iranpoor, N.; Khoshnood, A. Aluminum tris (dodecyl sulfate) trihydrate  $\text{Al}(\text{DS})_3 \cdot 3\text{H}_2\text{O}$  as an efficient Lewis acid–surfactant-combined catalyst for organic reactions in water. *J. Mol. Catal. A: Chem.* **2007**, *274*, 109–115.